JOURNAL OF SOLID STATE CHEMISTRY 97, 476–480 (1992)

BRIEF COMMUNICATIONS

Mechanism of Metal–Insulator Transition in the Systems $(Ln_{1-x}Ca_x)MnO_{3-\delta}$ (*Ln*: La, Nd, and Gd) and $(Nd_{0.1}Ca_{0.9-y}Sr_y)MnO_{2.97}$

H. TAGUCHI[1] AND M. NAGAO

Research Laboratory for Surface Science, Faculty of Science, Okayama University, Okayama 700, Japan

AND M. SHIMADA

Department of Molecular Chemistry and Engineering, Faculty of Engineering, Tohoku University, Sendai 980, Japan

Received July 24, 1991

The electrical resistivity (ρ) of the perovskite-type $(Ln_{1-x}Ca_x)MnO_{3-\delta}$ (*Ln*: La, Nd, and Gd) and $(Nd_{0.1}Ca_{0.9-y}Sr_y)MnO_{2.97}$ were measured in the temperature range 300 to 800 K. In the case of $(Ln_{1-x}Ca_x)MnO_{3-\delta}$ (*Ln*: La, Nd, and Gd), $d\rho/dT$ increases with increasing x. The increase of $d\rho/dT$ is explained by both the decrease in the Mn–O distance and the number of $3d$ electrons which exist in the conduction band. On the other hand, in the case of $(Nd_{0.1}Ca_{0.9-y}Sr_y)MnO_{2.97}$, $d\rho/dT$ decreases slightly with increasing y and corresponds to an increase in the Mn–O distance.

Introduction

$CaMnO_3$ has an orthorhombic perovskite-type structure, and the space group is *Pnma* (*1, 2*). $CaMnO_3$ exhibits a weak ferromagnetism with $T_N = 123$ K (*3*) and an *n*-type semiconductor (*4*). Many investigations have been reported on the substitution of Ca^{2+} ion by rare earth ion in $CaMnO_3$ (*3, 5, 6*). The electrical properties of $(Ln_{1-x}Ca_x)MnO_{3-\delta}$ (*Ln*: La, Nd, Gd, Tb, Ho, and Y) were measured by Taguchi *et al.* and Kobayashi *et al.* (*7–10*).

$(Ln_{1-x}Ca_x)MnO_{3-\delta}$ (*Ln*: La, Nd, Gd, Tb, Ho, and Y) exhibits *n*-type semiconducting behavior below room temperature. At low temperature, the electrical resistivity (ρ) follows Mott's $T^{-1/4}$ law, indicating the possible occurrence of variable range hopping of electrons due to Anderson localization (*11*). At high temperature, ρ of these manganates has a positive temperature coefficient, and the metal–insulator transition of these manganates occurs without any crystallographic change; $d\rho/dT$ of these manganates depends on x. The metal–insulator transition temperature (T_t) of these manganates decreases with increasing x. At a particular value of x, in which the Mn^{3+}/Mn^{4+} ratio is constant, T_t of these manganates increases with increasing average Mn–O distance (*10*).

The electrical properties of the perov-

[1] To whom correspondence should be addressed.

0022-4596/92 $3.00

skite-type $(Nd_{0.1}Ca_{0.9-y}Sr_y)MnO_{2.97}$ were measured (*12*). In $(Nd_{0.1}Ca_{0.9-y}Sr_y)MnO_{2.97}$, both the number of $4f$ electrons in the rare earth ion and the Mn^{3+}/Mn^{4+} ratio are independent of y. In the range $0 \leq y \leq 0.4$, the metal–insulator transition occurs. Both the cell constants and T_t linearly increase with increasing y. Since both the number of $4f$ electrons and $3d$ electrons are independent of y, it is considered that T_t depends on the Mn–O distance.

In the present study, we exactly measured $d\rho/dT$ of both $(Ln_{1-x}Ca_x)MnO_{3-\delta}$ (*Ln*: La, Nd, and Gd) and $(Nd_{0.1}Ca_{0.9-y}Sr_y)MnO_{2.97}$ at high temperature. The mechanism of the metal–insulator transition of these manganates and the effect of $d\rho/dT$, a band gap, T_t, and Mn–O distance are discussed.

Experimental

The preparation of $(Ln_{1-x}Ca_x)MnO_{3-\delta}$ (*Ln*: La, Nd, and Gd) and $(Nd_{0.1}Ca_{0.9-y}Sr_y)MnO_{2.97}$ was described in detail elsewhere (*7–9, 12*). For measuring the electrical resistivity, the powder manganates were pressed into a pellet form under a pressure of 50 MPa, and the pellet was sintered at 1623 K for 12 hr under the flow of pure oxygen gas. The oxygen-deficient materials obtained in this manner were annealed at 973 K under a flow of pure oxygen gas.

The electrical resistivity of the manganates was measured by a standard four-electrode technique in the temperature range 300 to 800 K.

Results and Discussion

At high temperature, the electrical resistivity (ρ) of $(Ln_{1-x}Ca_x)MnO_{3-\delta}$ (*Ln*: La, Nd, and Gd) linearly increases with temperature in the range $0.7 \leq x \leq 0.9$ for La, $0.6 \leq x \leq 0.9$ for Nd, and $0.7 \leq x \leq 0.9$ for Gd, respectively; ρ of $(Nd_{0.1}Ca_{0.9-y}Sr_y)MnO_{2.97}$ also linearly increases with temperature in the range $0 \leq y \leq 0.3$. At high temperature, ρ

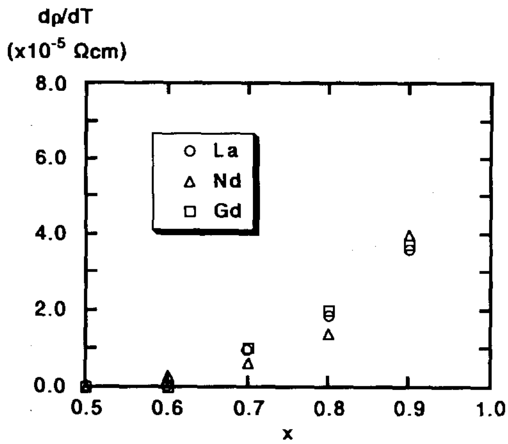

FIG. 1. $d\rho/dT$ vs x for the system $(Ln_{1-x}Ca_x)MnO_{3-\delta}$ (*Ln*: La, Nd, and Gd).

for the metallic materials linearly increases with increasing temperature and given by

$$\rho = \rho_o + \rho(T), \quad (1)$$

where ρ_o is a constant which increases with increasing impurity content and $\rho(T)$ is the temperature-dependent part of the electrical resistivity (*13*). $\rho(T)$ is given by

$$\rho(T) = \rho'\alpha T, \quad (2)$$

where ρ' is a constant, α is a temperature coefficient, and T is temperature (*14*). As we used the sintered manganates, ρ_o depends on the density of the manganates. On the other hand, ρ' depends on the composition of the manganates. In the present study, we used $d\rho/dT$ which is given by

$$d\rho/dT = \rho'\alpha, \quad (3)$$

because it is not easy to get ρ' and α independently. Figure 1 shows the relation between $d\rho/dT$ of $(Ln_{1-x}Ca_x)MnO_{3-\delta}$ (*Ln*: La, Nd, and Gd) and x; $d\rho/dT$ monotonously increases with increasing x with little difference between La, Nd, and Gd. Figure 2 shows the relation between $d\rho/dT$ of $(Nd_{0.1}Ca_{0.9-y}Sr_y)MnO_{2.97}$ and y. Though both the number of $4f$ electrons in the rare

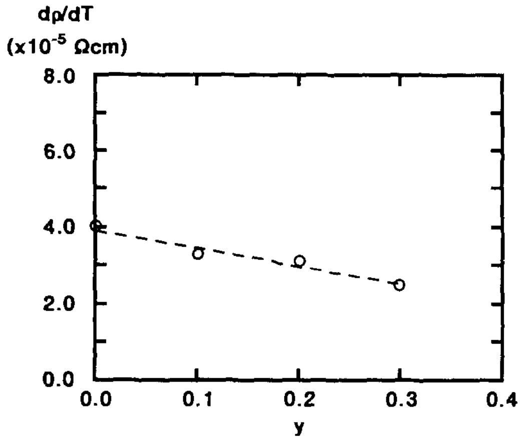

FIG. 2. $d\rho/dT$ vs y for the system $(Nd_{0.1}Ca_{0.9-y}Sr_y)MnO_{2.97}$.

earth ion and the Mn^{3+}/Mn^{4+} ratio are independent of y, $d\rho/dT$ slightly decreases with increasing y.

The characteristics of $(Ln_{1-x}Ca_x)MnO_{3-\delta}$ (*Ln*: La, Nd, and Gd) and $(Nd_{0.1}Ca_{0.9-y}Sr_y)MnO_{2.97}$ are summarized as follows (*7–9, 12*). The unit cell volume of $(Ln_{1-x}Ca_x)MnO_{3-\delta}$ (*Ln*: La, Nd, and Gd) decreases with increasing x. The decrease of the unit cell volume is explained by the decrease of the Mn^{3+} ion content, and the Mn–O distance decreases with increasing x. The unit cell volume of $(Nd_{0.1}Ca_{0.9-y}Sr_y)MnO_{2.97}$ slightly increases with increasing y. The increase of the unit cell volume is explained by the increase of Sr^{2+} ion content, and Mn–O distance slightly increases with increasing y. At low temperature, these manganates are *n*-type semiconductors and the relation between log ρ and $1/T$ is schematically shown in Fig. 3(A). With increasing x, the slope of log ρ–$1/T$ curves for $(Ln_{1-x}Ca_x)MnO_{3-\delta}$ (*Ln*: La, Nd, and Gd) decreases and the band gap (Δ) between the valence band and conduction band decreases. On the other hand as shown in Fig. 3(B), the slope of log ρ–$1/T$ curves for $(Nd_{0.1}Ca_{0.9-y}Sr_y)MnO_{2.97}$ slightly increase with increasing y, and Δ increases. Figure 4 schematically shows the changes in T_t with composition. Magnetic susceptibility measurement of the manganates suggests that the spin state of Mn^{3+} ion changes from low to high at T_t (*7–9*).

We propose a simple energy band scheme of which the valence band (π^* orbital) and the conduction band (σ^* orbital) are separated by Δ as shown in Fig. 5 which is

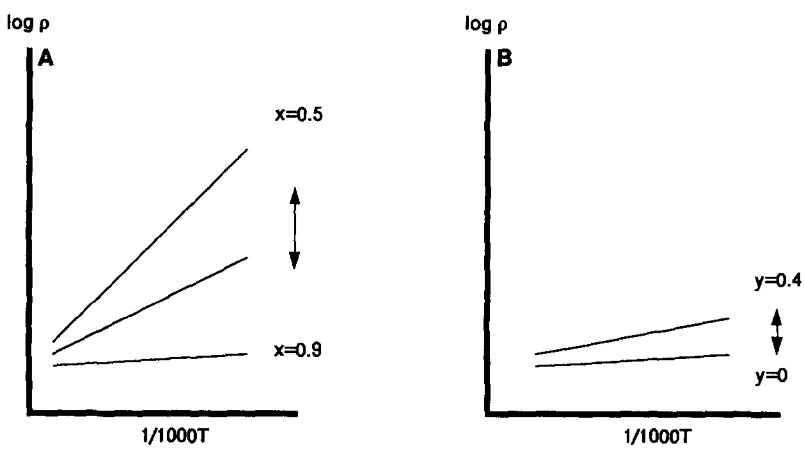

FIG. 3. Schematic illustration of log ρ vs $1/T$ for the systems [A] $(Ln_{1-x}Ca_x)MnO_{3-\delta}$ (*Ln*: La, Nd, and Gd) and [B] $(Nd_{0.1}Ca_{0.9-y}Sr_y)MnO_{2.97}$.

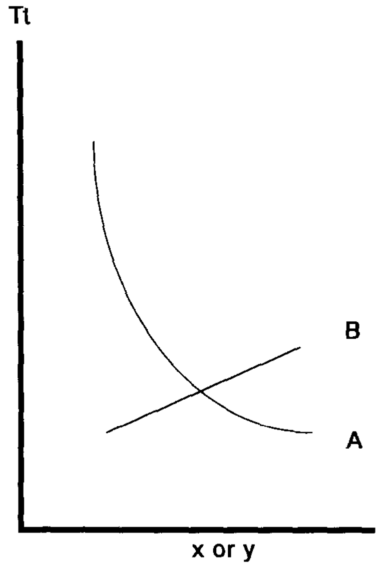

FIG. 4. Schematic illustration of T_t vs x or y for the systems [A] $(Ln_{1-x}Ca_x)MnO_{3-\delta}$ (Ln: La, Nd, and Gd) and [B] $(Nd_{0.1}Ca_{0.9-y}Sr_y)MnO_{2.97}$.

strongly affected by temperature, the number of $3d$ electrons, and the Mn–O distance. In the case of $(Ln_{1-x}Ca_x)MnO_{3-\delta}$ (Ln: La, Nd, and Gd), both the Mn–O distance and the number of $3d$ electrons decrease with increasing x, and Δ decreases. Because Δ is narrow when Mn^{4+} dominates, it is easy for the spin state of the Mn^{3+} ion to change from low to high at low temperature. Consequently, the metal–insulator transition occurs, and T_t decreases with increasing x. On the other hand in the case of $(Nd_{0.1}Ca_{0.9-y}Sr_y)MnO_{2.97}$, the number of $3d$ electrons is constant and only the Mn–O distance increases slightly with increasing y and Δ increases. It is therefore unfavorable for the spin state of Mn^{3+} ion to change from low to high at low temperature and consequently, T_t increases with increasing y. The present discussion gives a good agreement with the schematic illustration of experimental results shown in Fig. 4. Based on these results, it is clear that the Mn–O distance plays an important role to T_t; that is, T_t increases with increasing Mn–O distance.

Both the Mn–O distance and the number of $3d$ electrons are important factors that control $d\rho/dT$ above T_t. In the case of $(Ln_{1-x}Ca_x)MnO_{3-\delta}$ (Ln: La, Nd, and Gd), both the Mn–O distance and the number of $3d$ electrons decrease with increasing x. No difference was observed in $d\rho/dT$–x relation for La, Nd, and Gd (see in Fig. 1.) because the number of $3d$ electrons does not depend on the Ln ion. The number of the $3d$ electrons which exist in the conduction band decreases with increasing x, and $d\rho/dT$ increases with increasing x. From these results, it is concluded that both the Mn–O distance and the number of $3d$ electrons play an important role in determining $d\rho/dT$. On

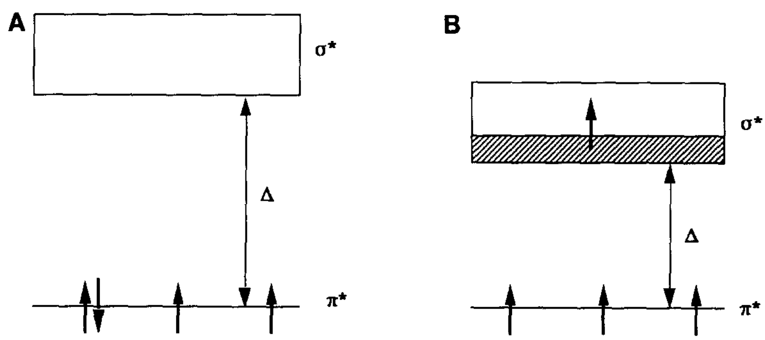

FIG. 5. Schematic illustration of the energy band for the systems $(Ln_{1-x}Ca_x)MnO_{3-\delta}$ (Ln: La, Nd, and Gd) and $(Nd_{0.1}Ca_{0.9-y}Sr_y)MnO_{2.97}$. [A] is below T_t and [B] is above T_t.

the other hand, in case of $(Nd_{0.1}Ca_{0.9-y}Sr_y)MnO_{2.97}$, the Mn–O distance increases slightly with increasing y, but the number of 3*d* electrons is constant. Though the number of the 3*d* electrons which exist in the conduction band is constant, $d\rho/dT$ slightly decreases with increasing y, as shown in Fig. 2. From these results, it is concluded that the small decrease in $d\rho/dT$ is caused by the increase of the Mn–O distance.

Conclusion

The band gap, Δ, which is affected by Mn–O distance and the number of 3*d* electrons, directly affects the metal–insulator transition in $(Ln_{1-x}Ca_x)MnO_{3-\delta}$ (*Ln*: La, Nd, and Gd) and $(Nd_{0.1}Ca_{0.9-y}Sr_y)MnO_{2.97}$. In the case of $(Ln_{1-x}Ca_x)MnO_{3-\delta}$ (*Ln*: La, Nd, and Gd), both the Mn–O distance and the number of 3*d* electrons decrease with increasing x whereby Δ decreases with increasing x and the spin state of Mn^{3+} ion easily changes from low to high. Consequently, the metal–insulator transition occurs, and T_t decreases with increasing x. Above T_t, $d\rho/dT$ increases with a decrease in both the Mn–O distance and the number of 3*d* electrons in the conduction band.

In contrast, in the case of $(Nd_{0.1}Ca_{0.9-y}Sr_y)MnO_{2.97}$, the number of 3*d* electrons is constant and Δ increases slightly with increasing Mn–O distance. It is unfavorable for the spin state of Mn^{3+} ion to change from low to high at low temperature. Consequently, T_t increases with increasing y and above T_t, the slight increase in the Mn–O distance causes the decrease of $d\rho/dT$.

References

1. K. R. Poeppelmeier, M. E. Leonowicz, J. C. Scanlon, J. M. Longo, and W. E. Yelon, *J. Solid State Chem.* **45**, 71 (1982).
2. H. Taguchi, M. Nagao, T. Sato, and M. Shimada, *J. Solid State Chem.* **78**, 312 (1989).
3. J. B. MacChesney, H. J. William, J. F. Potter, and R. C. Sherwood, *Phys. Rev.* **164**, 779 (1967).
4. H. Taguchi, *Phys. Status Solidi A* **88**, K79 (1985).
5. G. H. Jonker and J. H. Van Santen, *Physica* **16**, 337 (1950).
6. G. H. Jonker, *Physica* **22**, 707 (1956).
7. H. Taguchi, and M. Shimada, *J. Solid State Chem.* **62**, 290 (1986).
8. H. Taguchi, M. Nagao, and M. Shimada, *J. Solid State Chem.* **76**, 284 (1988).
9. H. Taguchi, M. Nagao, and M. Shimada, *J. Solid State Chem.* **82**, 8 (1989).
10. T. Kobayashi, H. Takizawa, T. Endo, T. Sato, M. Shimada, H. Taguchi, and M. Nagao, *J. Solid State Chem.* **92**, 116 (1991).
11. N. F. Mott, *Adv. Phys.* **21**, 785 (1972).
12. H. Taguchi, M. Nagao, and M. Shimada, *J. Solid State Chem.* **92**, 227 (1991).
13. A. J. Dekker, "Solid State Physics," p. 288, Prentic–Hall, New York (1957).
14. T. Tanaka, "Electronic and Communications Materials," p. 62, Korona-sha, Tokyo (1981) [in Japanese].